JOURNAL OF APPLIED ELECTROCHEMISTRY 25 (1995) 358–363

Influence of temperature on electroreduction of anodically formed passive films on lead electrodes in H_2SO_4 solutions
Part I: Electroreduction of $PbSO_4$ layers

F.E. VARELA, L.M. GASSA, J.R. VILCHE*

Instituto de Investigaciones Fisicquímicas Teóricas y Aplicadas (INIFTA), Facultad de Ciencias Exactas, Universidad Nacional de La Plata, Sucursal 4, C.C. 16, (1900) La Plata, Argentina

Received 12 April 1994; revised 12 June 1994

Combined voltammetry and potentiostatic current transient techniques have been employed to study the electroreduction processes of anodically formed lead sulphate layers on polycrystalline lead electrodes in concentrated sulphuric acid solutions in the 0–50° C temperature range. Data analysis using parametric identificiation procedures and nonlinear fit routines has demonstrated that the kinetics of the electroreduction processes of the Pb(II)-containing surface species can be interpreted in terms of complex nucleation and growth mechanisms. The electroreduction of the $PbSO_4$ layer involves mainly an instantaneous nucleation and 3D growth mechanism under diffusion control. The activation energy of the different reaction stages can be calculated from Arrhenius plots derived from the corresponding kinetic parameters. This contributes to a better understanding of the whole cathodic reaction scheme as well as to the identification and characterization of the various stages taking place in the electroreduction processes.

1. Introduction

The lead–acid battery is one of the most successful electrochemical energy storage systems, but is open to new developments to improve its performance. Accordingly, many attempts have been made to study the anodic dissolution of lead in aqueous sulphuric acid solutions and to establish the properties of passive layers [1, 2], particularly in order to determine the composition and structure of the surface film which is formed on the negative electrode of lead–acid cells under anodic oxidation conditions [3–7]. The kinetics and mechanisms of the cathodic reactions taking place during the charge stages of lead (Pb) electrodes have received considerably less attention and, in general, conclusions are more difficult to arrive at than the case of lead electrooxidation.

The electroreduction of $PbSO_4$ has been investigated by using the potential sweep method [8] with the corresponding kinetics assumed to be controlled by the diffusion of Pb^{2+} ions to the reaction sites located at the interface between the Pb and the $PbSO_4$ crystals. The effects of crystal size, solubility, diffusion coefficient, and length of the diffusion path on the reduction of lead sulphate were examined within the frame of a microscopic reaction site model [8, 9]. On the other hand, the potentiostatic electroreduction of $PbSO_4$ has recently been investigated at 25° C, and kinetic results have been interpreted mainly by an instantaneous nucleation and 3D growth mechanism under diffusion control [10].

It is worth noting that, in contrast to the large number of investigations concerning the electrochemical behaviour of lead in H_2SO_4 solutions at room temperature, there are comparatively few studies on the influence of temperature on the electrode kinetics. Nevertheless, from the effect of variable temperature on the performance of the lead–acid battery it has been concluded that failures at low temperature operation are due to either the irreversible sulphation of a few positive plates or the morphological changes in the active material of the positive electrode, whereas at high temperatures the positive plate composition appears to be more uniform throughout the device and failures can be associated with negative plate deterioration and/or corrosion of positive grids [11, 12]. The beneficial effects of additives, usually known as expanders, have been studied to promote the oxidation of lead in H_2SO_4 in order to enhance its performance at low temperature [13]. Otherwise, according to the activation energies and entropies of diffusion reported in a study of the oxidation kinetics of anodic films on lead in H_2SO_4 in the −50 to 0° C temperature range, the desorption of water or dehydration of ions play an important role in the activation process [14]. Several studies of temperature effects on the positive electrode behaviour have been reported [15–18]. It should be noted that the

* To whom correspondence should be addressed

0021-891X

standard $Pb/PbSO_4$, H_2SO_4 electrode potential over the 20–240° C range has been described by a simple relationship, including a temperature coefficient of about $-1.26\,mV\,K^{-1}$ [19], although a value of $-1.015\,mV\,K^{-1}$ has also been reported [20].

The aim of this paper is to analyse the influence of temperature on the electroreduction of anodic layers formed on lead in H_2SO_4 solution in order to postulate an appropriate nucleation and growth mechanism to interpret the kinetics of data concerning this electrode reaction in the 0–50° C temperature range. This offers the possibility of evaluating to what extent kinetic models derived from single Pb(II)-containing films at room temperature can be applied to the electroreduction of composite lead sulphate-oxide passive layers, covering a wide temperature range.

2. Experimental details

The experimental setup was described in previous publications [2, 6, 10]. High purity polycrystalline lead ('Specpure', Johnson Matthey Chemicals Ltd, $0.30\,cm^2$ apparent area) in the form of discs embedded in PTFE holders were used as working electrodes in 5M H_2SO_4. The electrolyte solution was prepared from analytical grade (p.a. Merck) reagents and triply distilled water. Potentials were measured and are referred to in the text against a Hg/Hg_2SO_4, K_2SO_4 (sat.) reference electrode (0.680 V on the NHE scale).

Prior to the electrochemical experiments the working electrodes were mechanically polished with a 600 grade emery paper, thoroughly rinsed with triply distilled water and cathodically polarized for $\tau_0 = 5$ min at −1.30 V, i.e., in the hydrogen evolution reaction potential range, to achieve a reproducible electroreduced lead surface. Runs were performed under nitrogen gas saturation at temperatures (T) in the 0–50° C range using the following potential programs: (i) single (STPS) or repetitive (RTPS) triangular potential sweeps which were applied at convenience between preset cathodic ($E_{s,c}$) and anodic ($E_{s,a}$) switching potentials at a scan rate (v) in the $0.002\,V\,s^{-1} \leqslant v \leqslant 0.200\,V\,s^{-1}$ range; and (ii) STPS or RTPS combined with potential steps, usually two potential steps covering different fixed potential regions. The first potential step ($E_i = E_{s,a} = -1.00$ V) was applied for a time $\tau = 3$ min to modify the anodically formed passive layer in order to change the total amount of anodic surface products, whereas the second potential step (E_f) was set sufficiently negative to electroreduce the anodic layer, usually $E_f < -1.05$ V, the corresponding current transients being systematically recorded.

3. Results and discussion

3.1. *Voltammetric data*

The voltammograms of lead in 5M H_2SO_4 at $v = 0.02\,V\,s^{-1}$ run between $E_{s,c} = -1.30$ V and $E_{s,a} = 0.40$ V at different temperatures are shown in Fig. 1(a). The potentiodynamic response exhibits an anodic peak A1 attributed to the oxidation of Pb to Pb(II) species and two cathodic current contributions, which can be associated with the electroreduction of PbO (peak C2) and $PbSO_4$ (peak C1) layers, respectively. The cathodic charge density related to the electroreduction of PbO species strongly depends on $E_{s,a}$, so that for $E_{s,a} \leqslant -0.40$ V [2] the current peak C2 practically disappears (see, for instance Fig. 1(b) for $E_{s,a} = -0.80$ V). The influence of temperature on the current density/potential (j/E) profiles can be clearly seen in the gradual change of the electrochemical response leading to a progressive deactivation of the electrooxidation and electroreduction processes as temperature is lowered, causing a decrease in the voltammetric charge density related to both peaks A1 and C1.

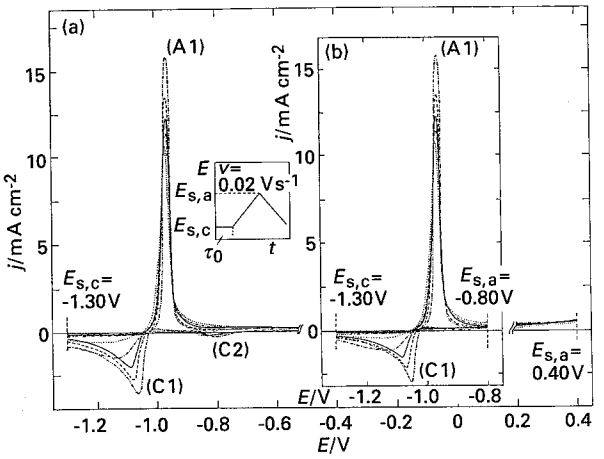

Fig. 1. Voltammograms of lead (Pb) run at $v = 0.02\,V\,s^{-1}$ between $E_{s,c} = -1.30$ V and $E_{s,a} = 0.40$ V (a) or $E_{s,a} = -0.80$ V (b) in 5M H_2SO_4. T: (···) 0, (– · – · –) 10, (——) 25, (– – – –) 35 and (– ·· – ·· –) 45° C.

From voltammograms run at constant v and different temperatures, linear $\log j_{p,C1}$ against T^{-1} (Fig. 2(a)) and $\log j_{p,C1}T^{1/2}$ against T^{-1} (Fig. 2(b)) plots are obtained, the corresponding slopes being about -1.46×10^3 and -1.53×10^3 K decade, respectively. From the former value it is possible to calculate an activation energy of about $28.1\,kJ\,mol^{-1}$. However, the linear dependence found for data presented in Fig. 2(b) can be tentatively assigned to a process under diffusion control (see also the linear $j_{p,C1}$ against $v^{1/2}$ relationship [21] discussed in Fig. 4(b) of [10] according to data obtained at room temperature). Therefore, an activation enthalpy close to $58.6\,kJ\,mol^{-1}$ can be estimated and, consequently, the experimental results obtained for the electroreduction process of $PbSO_4$ layers under potentiodynamic conditions can be explained by taking into account a reaction mechanism controlled by diffusion of Pb(II) ions through the surface film [13]. This conclusion will be confirmed from the analysis of potentiostatic current transients.

It is worth noting that the difference between the potentials of peaks A1 and C1, $\Delta E_p = E_{p,A1} - E_{p,C1}$, increases as the temperature decreases. This fact might be due to the shift of $E_{p,C1}$ to more negative

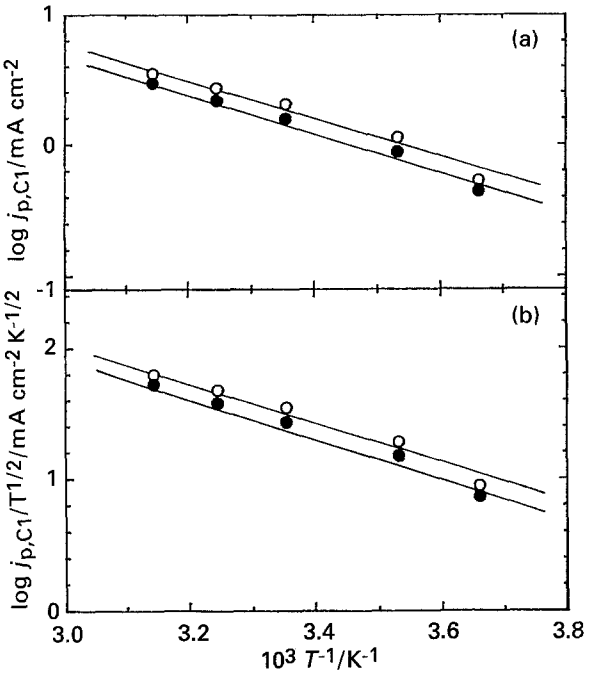

Fig. 2. Dependence of (a) $\log(j_{p,C1})$ and (b) $\log(j_{p,C1}T^{1/2})$ on T^{-1}. Data related to voltammograms shown in Fig. 1. Key: (●) $E_{s,a} = -0.8$ V, (○) +0.4 V.

potentials, since $E_{p,A1}$ seems to be independent of temperature in the range studied. This increase in ΔE_p, which can be related to an increasing irreversibility of the system, explains the dropping efficiency during the charge–discharge cycles of the Pb/$PbSO_4$ electrode at low temperatures. Recently, X-ray data have revealed that electrochemically formed $PbSO_4$ remains partly on the lead electrode surface even at high negative potentials, i.e., −1.5 V [22]. Furthermore, *in situ* i.r. spectroscopy results have pointed out that the i.r. band area, corresponding to the vibrational mode of the sulphate anion in the solid lead sulphate, does not attain the expected zero value during hydrogen evolution [23]. Accordingly, it can be assumed that the amount of relatively more stable $PbSO_4$ species increases with decreasing temperature, in agreement with the experimentally observed lesser amount of voltammetric charge involved in peak C1.

On the other hand, it should be noted that voltammograms run at 45° C when $E_{s,a}$ is located at both 0.40 V (Fig. 1(a)) and −0.80 V (Fig. 1(b)) exhibit, in the course of the reverse potential scan, a reactivation of the electrooxidation process at ca. −1.00 V (i.e., at potentials more positive than $E_{p,C1}$). Nevertheless, this reactivation (anodic current) peak diminishes remarkably as temperature decreases and it appears ill-defined when $T < 25$° C. Likewise, the reactivation of the anodic process observed at high temperature can be explained by considering the surface film rupture generated by internal stress due to decreasing electrostiction pressure as the potential becomes more negative. Therefore, the inner part of the film loses contact at some points of the electrode surface. This promotes the formation of small cracks which lead to a reoxidation of the exposed lead at the bottom of fissures [24]. Local depassivation as a consequence of surface film breakdown during the cathodic charging of lead electrodes has been detected by *in situ* i.r. external reflection–adsorption spectroscopy [23].

3.2. *Electroreduction current transients*

Potentiostatic current transients corresponding to the electroreduction of $PbSO_4$ layers formed on lead in H_2SO_4 solutions at different temperatures by a linear potential scan between $E_{s,c} = -1.30$ V and $E_i = E_{s,a}$ set in the peak A1 potential range at $v = 0.02$ V s^{-1} were studied at values of E_f ranging from −1.06 to −1.20 V. The electroreduction process at E_f was preceded by a potential step during $\tau = 3$ min at $E_i = -1.00$ V, which is remarkably more negatively located than the potential region of PbO layer formation.

The experimental current transients can be satisfactorily reproduced through the expression [10]

$$j(t) = P_1 t^{-1/2}[1 - \exp(-P_2 t)] + P_3 t^{-1/2} \quad (1)$$

The first term in Equation (1) corresponds to an instantaneous nucleation and 3D growth process under diffusion control [25]. In this case,

$$P_1 = zFD_j^{1/2}\Delta c_j \pi^{-1/2} \quad (2)$$

and

$$P_2 = N_0 \pi K_j D_j \quad (3)$$

where K_j denotes a proportionality constant, $K_j = (8\pi\Delta c_j M\rho^{-1})^{1/2}$, D_j and Δc_j are the diffusion coefficient and the concentration difference, respectively, of the diffusing j-species across the Nernst diffusion layer, N_0 are the nuclei instantaneously formed, M is the molecular weight of $PbSO_4$ and ρ is the density of the surface layer.

The second term in Equation 1, which stands for the initial falling current transient corrected for the electrical double layer discharge, can be related to an instantaneous nucleation and 2D growth under diffusion control [26]. P_3 is explicitly given by the following relationship

$$P_3 = zFD_i^{1/2}\Delta c_i \pi^{-1/2} \quad (4)$$

where D_i and Δc_i are the diffusion coefficient and concentration difference of the mobile species i inside the solution in pores of the surface film.

The good agreement at different temperatures between the experimental results obtained at $E_i = -1.00$ V ($\tau = 3$ min) and $E_f = -1.085$ V and data calculated from Equation 1 is presented in Fig. 3. Although the shape of current transients is similar to that found in previous work at 25° C [10], with decreasing temperature a deactivation of the electroreduction process can be clearly observed, whereas the value of the peaked current density j_M diminishes and the time t_M becomes longer. Furthermore, Fig. 3 shows that at 0° C no current maximum is found in the

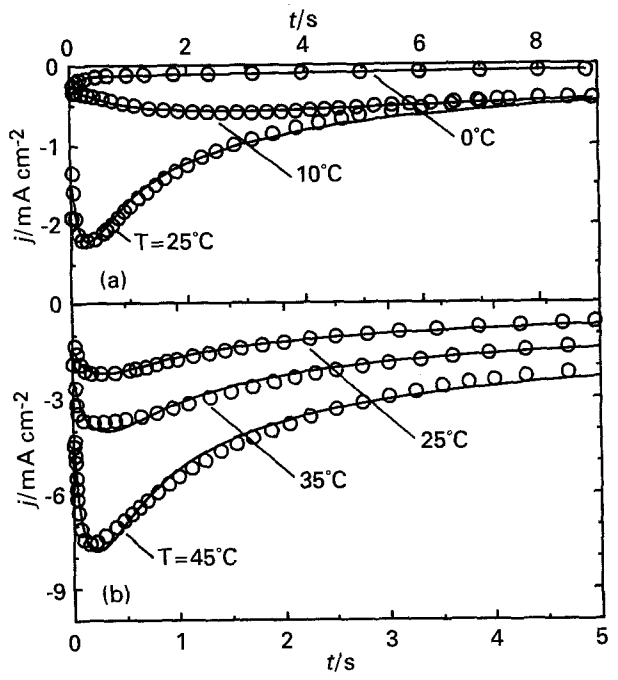

Fig. 3. Fitting of current transient data recorded at different temperatures and $E_f = -1.085$ V after a potential holding at $E_i = -1.00$ V during $\tau = 3$ min, according to Equation 1 (full traces).

cathodic current transient at $E_f = -1.085$ V. Thus, in order to detect a well defined j_M value it is necessary to set E_f more negatively as temperature decreases. This behaviour can be easily related to the shift of $E_{p,Cl}$ observed in the voltammograms (see, for instance Fig. 1).

The set of adjusted parameters exhibits linear P_1 against E_f (Fig. 4(a)) and P_2 against E_f (Fig. 4(b)) relationships whose slopes increase with increasing temperature. The E_f value at which the electroreduction of $PbSO_4$ starts (from extrapolations of $P_1 \rightarrow 0$ and $P_2 \rightarrow 0$) shifts to more negative potentials as

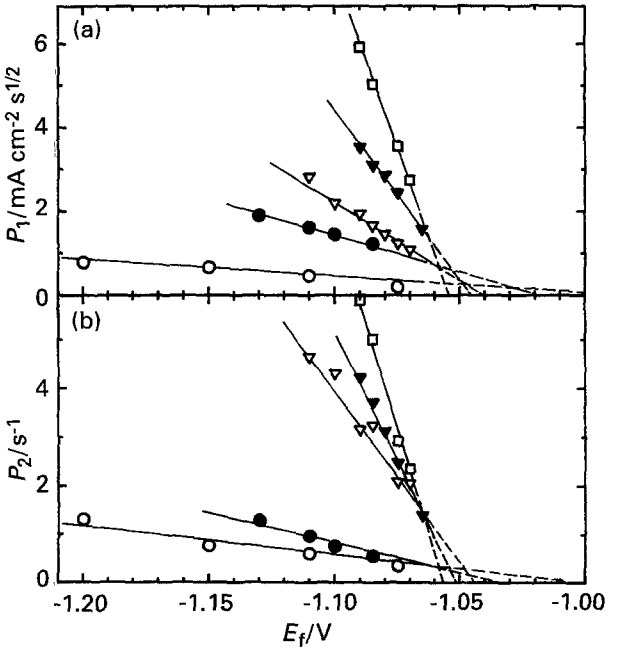

Fig. 4. Dependence of (a) P_1 and (b) P_2 on E_f for different temperatures in the $0° C \leqslant T \leqslant 45° C$ range. $E_i = 1.00$ V. T: (□) 45, (▼) 35, (▽) 25, (●) 10 and (○) 0° C

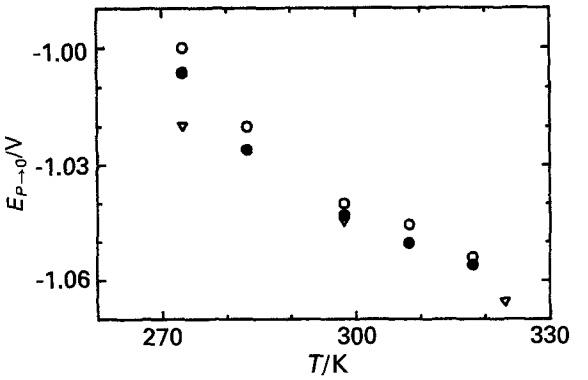

Fig. 5. Temperature influence on $E_{P\rightarrow 0}$. Data related to P_1 and P_2 parameter dependences with E_f shown in Fig. 4, and calculated values of E_r from Equation 6. Key: (○) P_1, (●) P_2 and (▽) values from Equation 6.

the system temperature coefficient approaches -1.1 mV K^{-1}. This value is very close to that reported in the literature [19, 20] taking into account that at fixed temperature $E_{P\rightarrow 0}$ can be compared to the reversible potential of the electrode reaction according to a Nernst equation. Let us consider the following possible consecutive reactions involved in the Pb(II)-sulphate layer electroreduction mechanism:

$$PbSO_4 + H_3O^+ \rightleftharpoons Pb^{2+} + HSO_4^- + H_2O \quad (5a)$$

$$Pb^{2+} + 2e^- \rightleftharpoons Pb \quad (5b)$$

The set of reactions (5) implies a phase transition process, whose kinetics can be interpreted by a nucleation and 3D growth mechanism under diffusion control, so that H_3O^+/HSO_4^- or Pb^{2+} ions migrate alternately through the $PbSO_4$ layer. Therefore, taking into account that the reaction scheme includes a fast electron transfer in the reaction step (5b), the concentration of active ions at the $Pb/PbSO_4$ interface depends on E_f. Assuming that the activity of solid species ($PbSO_4$ and Pb) is unity, the local reversible potential which is established at the onset of the electroreduction current ($E_{P\rightarrow 0}$), can be expressed by

$$E_r = E^0 + \frac{RT}{2F} \ln a_{Pb^{2+}} \quad (6a)$$

Under equilibrium conditions, the concentration of Pb^{2+} is determined by the solubility product (K_s) of $PbSO_4$ at fixed temperature, and accordingly

$$E_r = E^0 + \frac{RT}{2F} \frac{\ln K_s}{a_{SO_4^{2-}}} \quad (6b)$$

Calculated values of E_r at 0, 25, and 50° C based on data of E^0 [20], K_s [27] and SO_4^{2-} ion concentration in 5M H_2SO_4 measured by Raman spectroscopy [28], are shown in Fig. 5. Small discrepancies between experimental $E_{P\rightarrow 0}$ and calculated E_r values can be justified, in principle, by the use of concentrations instead of the ion activities. The electroreduction mechanism given by Reactions 5(a) and (b) should be considered as an example to interpret the value expected for the temperature coefficient of E_r. A further insight in the reaction pathway requires more information on the identity of diffusion-controlling species. It should be mentioned that in concentrated

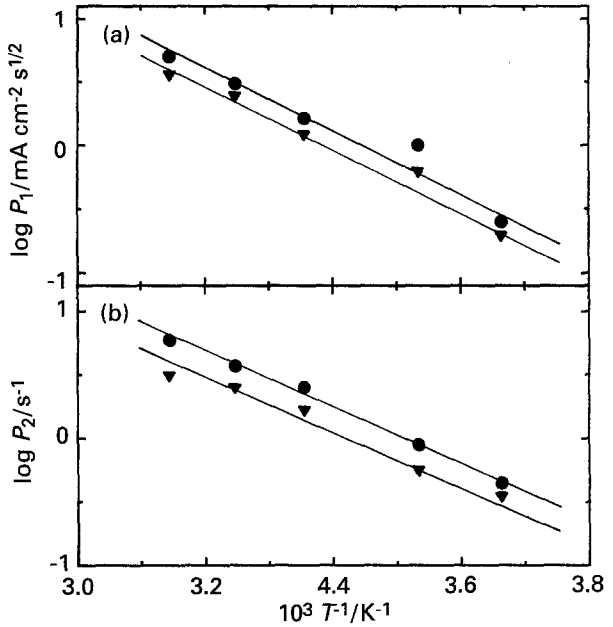

Fig. 6. Dependence of (a) P_1 and (b) P_2 on temperature. Data related to current transients obtained at different temperatures and $E_f = -1.085$ V (●) or $E_f = -1.075$ V (▼) after a potential holding at $E_i = -1.00$ V during $\tau = 3$ min.

sulphuric acid solutions several soluble Pb(II)-containing complexes, i.e., $PbHSO_4^+$, besides Pb^{2+} ions must be considered [29].

The linear dependence of P_1 on E_f is not directly expected for a simple diffusion process, and it can be tentatively attributed to the dependence of Δc_j on E_f and, to a minor extent to changes of D_j according to E_f. The concentration difference Δc_j denotes the driving force of a mass transfer controlled process [25], which can be expressed as $\Delta c_j = c_j^b - c_j^s$ the difference between bulk and surface concentrations, respectively. In such a case, if consecutive reaction steps (5a) and (5b) represent the reaction mechanism, c_j^b can be assigned, in principle, to dissolving Pb^{2+} ions generated in step (5a), whose concentration depends on the $PbSO_4$ solubility in the acid media although it is independent of potential, and c_j^s denotes the surface concentration of Pb^{2+} ions which is electrode potential dependent following a Nernst equation. Thus, as E_f is set more negatively Δc_j should increase and P_1 become greater. Likewise, with decreasing E_f the value of $c^s_{Pb^{2+}}$ in the vicinity of the lead surface diminishes and, accordingly, as $c^b_{Pb^{2+}}$ is almost constant at each temperature, Δc_j increases. The fact that some electrochemically inert $PbSO_4$ species still remains on the lead surface [22] gives support to a constant value of $c^b_{Pb^{2+}}$ during the electroreduction process.

Figure 6 presents $\log P_i (i = 1, 2)$ against $1/T$ Arrhenius plots corresponding to data derived from measurements at $E_f = -1.085$ V and $E_f = -1.075$ V. Assuming that the diffusion coefficient obeys the typical relationship predicted from the theory of absolute reaction rate [30], then

$$D_j = e\lambda^2 (kT/h) \exp(\Delta S^*/R) \exp(-\Delta H^*/RT) \quad (7a)$$

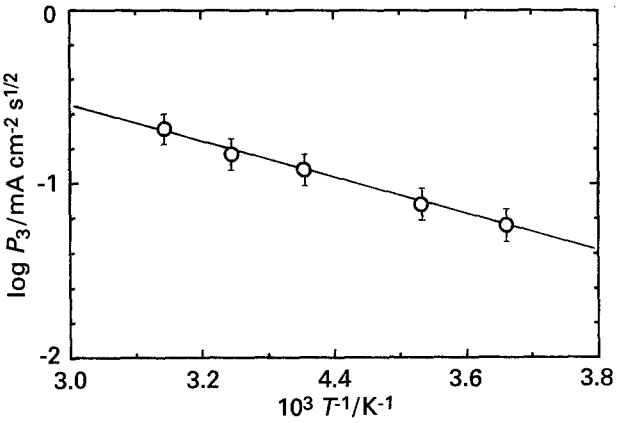

Fig. 7. Dependence of P_3 on temperature. Data related to current transients obtained at different temperatures and E_f within the $PbSO_4$ electroreduction potential range after a potential holding at $E_i = -1.00$ V during $\tau = 3$ min.

where e is the base of natural logarithms and λ, the 'jump distance', the distance between successive equilibrium positons, ΔS^* and ΔH^* are the molar activation entropy and enthalpy, respectively. The other symbols have their usual meaning. To account for an Arrhenius relationship the preexponential factor can be neglected and Equation 7(a) becomes

$$D_j = D_j^0 \exp(-\Delta H^*/RT) \quad (7b)$$

Thus, from the slope of $\Delta \log P_1/\partial(1/T)$ plots (Fig. 6) and taking into account the general expressions given in Equations 2 and 7(b), it is possible to calculate an activation enthalpy for the diffusion coefficient D_j of about $\Delta H^*_{D_j} = 95.7 \pm 0.4$ kJ mol^{-1}. This value is in close agreement with that found by Valeriote *et al.* [14] during the oxidation of anodic films on lead in sulphuric acid solutions at low temperatures, where the rate-limiting diffusion of ions may be controlled by an activation process involving partial dehydration of the diffusing ion and/or desorption of interfacial water. Otherwise, the P_2 parameter involves, in principle, two strongly temperature-dependent components, which are D_j and N_0. As in the case of N_0 an Arrhenius behaviour is expected and $\Delta H^*_{D_j}$ is already known, from the slope $\partial \log P_2/\partial(1/T)$, the activation enthalpy of the active sites can be estimated.

The fitted P_3 parameter is practically constant at each temperature in the whole E_f range covered in this work. Likewise, the corresponding Arrhenius plot reveals that a linear $\log P_3$ against $1/T$ relationship is clearly obtained (Fig. 7). From its slope, $\Delta H^*_{D_i}$ is close to 40.2 kJ mol^{-1}. This value, which was found to be larger than that expected for an ion diffusion process in solution [31], supports the conclusion of previous work that P_3 in Equation 1 can be related to the diffusion controlled reversible electroreduction of Pb(II) ions from the supersaturated solution within the pores generated between the $PbSO_4$ crystals [10]. Therefore, the second term in Equation 1 which corresponds mainly to the initial short range cathodic current decay can be associated with the electroreduction of Pb(II) ions whose concentration under critical supersaturation conditions [32], can

attain a value of about 1.4×10^{-6} mol cm^{-3} during the $PbSO_4$ electroformation. This conclusion is consistent with the value $D_i \approx 10^{-6}$ cm^2 s^{-1} calculated from P_3 (Fig. 7) and the concentration of Pb(II) soluble species in the supersaturated solution in the pores at 25° C. The analysis of voltammetric results yields some information concerning the electroreduction of the $PbSO_4$ layer but it is unable to provide data directly related to the small cathodic contribution due to the electroreduction of Pb(II) ions located in pores.

Recently [6, 7], it has been shown that the $PbSO_4$ electroformation and subsequent passivation of the lead electrode can be described by a complex reaction model, which implies the formation of a thin ionically conducting film which assists the migration of Pb^{2+} ions and blocks the access of SO_4^{2-} to the interfacial region. Thus, due to the fact that Pb^{2+} ions are transferred to this film, the concentration of hydrated Pb^{2+} ions is increased, and highly crystalline $PbSO_4$ precipitate passivates the electrode.

4. Conclusions

The kinetic data analysis suggests that the nucleation and growth mechanism developed earlier to interpret the electroreduction of $PbSO_4$ at room temperature, can be successfully used in the 0 to 45° C temperature range.

The electroreduction processes of the primary $PbSO_4$ layer involve mainly an instantaneous nucleation and 3D growth mechanism under diffusion control. The reaction proceeds via the dissolution of lead sulphate followed by the diffusion of Pb(II) ions to the electrode surface (the rate-determining step) and a fast electron-transfer step. The initial falling current transient can be attributed to a mass transfer contribution due to the electroreduction of Pb(II) ions present as a supersaturated solution in the pores formed during the previous $PbSO_4$ layer growth.

The electroreduction process of the $PbSO_4$ layer becomes hindered as the temperature decreases. The dependence of this cathodic reaction on temperature is explained phenomenologically on the basis of the Arrhenius behaviour of the kinetic parameters involved in each reaction step. The activation energy estimated from the temperature dependence of the fitted parameters are in agreement with the diffusion processes involved in the reaction mechanism used to interpret the $PbSO_4$ electroreduction at 25° C.

Acknowledgements

This research project was financially supported by the Consejo Nacional de Investigaciones Científicas y Técnicas, The Comisión de Investigaciones Científicas de la Provincia de Buenos Aires, and the Fundación Antorchas. Part of the equipment used in the present work was provided by the DAAD and the Alexander von Humboldt-Stiftung.

References

[1] K. R. Bullock and D. Pavlov (eds), 'Advances in Lead–Acid Batteries', The Electrochemical Society, Pennington, NJ (1984).
[2] F. E. Varela, L. M. Gassa and J. R. Vilche, *J. Electroanal. Chem.* **353** (1993) 147.
[3] D. Pavlov, *Electrochim. Acta* **23** (1978) 845.
[4] D. Pavlov and N. Iordanov, *J. Electrochem. Soc.* **117** (1970) 1103.
[5] D. Pavlov, S. Zanova and G. Papazov, *ibid.* **124** (1977) 1522.
[6] F. E. Varela, M. E. Vela, J. R. Vilche and A. J. Arvia, *Electrochim. Acta* **38** (1993) 1513.
[7] F. E. Varela, J. R. Vilche and A. J. Arvia, *Electrochim. Acta*, in press.
[8] K. Kanamura and Z. Takehara, *J. Electrochem. Soc.* **139** (1992) 345.
[9] P. Ekdunge, K. V. Rybalka and D. Simmonson, *Electrochim. Acta* **32** (1987) 659.
[10] F. E. Varela, L. M. Gassa and J. R. Vilche, *ibid.* **37** (1992) 1119.
[11] D. C. Constable, J. R. Gardner, K. Harris, R. J. Hill, D. A. J. Rand and L. B. Zalcman, *J. Electroanal. Chem.* **168** (1984) 395.
[12] T. F. Sharpe and R. S. Conell, *J. Appl. Electrochem.* **17** (1987) 789.
[13] P. J. Mitchell, N. A. Hampson and J. Smith, *ibid.* **12** (1982) 13.
[14] E. M. L. Valeriote and L. D. Gallop, *J. Electrochem. Soc.* **124** (1977) 370, 380.
[15] M. Fleischmann and H. R. Thirsk, *Trans. Faraday Soc.* **51** (1955) 71.
[16] E. Hämeenoja, T. Laitinen, J. P. Phol, G. Sundholm and A. Yli-Pentii, 38th ISE meeting, Ext. Abstr. II, Maastricht (1987) p. 703.
[17] E. Hämeenoja, T. Laitinen, G. Sundholm and A. Yli-Pentii, *Electrochim. Acta* **34** (1989) 233.
[18] T. Laitinen and J. P. Phol, *ibid.* **34** (1989) 377.
[19] F. Letowski and G. Pinard-Legry, *ibid.* **26** (1981) 245.
[20] Z. Galus, *in* 'Standard Potentials in Aqueous Solution' (edited by A. J. Bard, R. Parsons and J. Jordan), Marcel Dekker, New York (1985) pp. 220–235.
[21] A. J. Bard and L. R. Faulkner, 'Electrochemical Methods', John Wiley & Sons, New York (1980).
[22] Y. Guo, J. Chen and L. Li, *J. Electrochem. Soc.* **139** (1992) L99.
[23] G. L. J. Trettenhahn, G. E. Nauer and A. Neckel, *Ber. Busenges. Phys. Chem.* **97** (1993) 422.
[24] F. E. Varela and J. R. Vilche, in preparation.
[25] B. R. Scharifker and J. Mostany, *J. Electroanal. Chem.* **117** (1984) 13.
[26] R. D. Armstrong and J. A. Harrison, *J. Electrochem. Soc.* **116** (1969) 328.
[27] 'Handbook of Chemistry and Physics', 67th edn., CRC Press, Boca Raton, Florida (1987).
[28] W. J. Hamer (ed.), 'The Structure of Electrolytic Solutions', John Wiley & Sons, New York (1959) pp. 48–55.
[29] A. N. Fleming, J. A. Harrison and J. Thompson, 'Power Sources 5', (edited by D. H. Collins), Academic Press, London (1975) p. 1.
[30] S. Glasstone, K. J. Laider and H. Eyring, 'The Theory of Rate Processes', McGraw-Hill, New York (1941) p. 524.
[31] H. R. Bruins, *in* 'International Critical Tables of Numerical Data, Physics, Chemistry and Technology' (edited by E. W. Washburn), Vol. V, McGraw-Hill, New York (1929) pp. 63–75.
[32] L. M. Baugh, K. L. Bladen and F. L. Tye, *J. Electroanal. Chem.* **145** (1983) 355.